



# Maximizing the information throughput of ultra-wideband fiber-optic communication systems

NIKITA A. SHEVCHENKO,<sup>\*</sup>  SAM NALLAPERUMA,  
AND SEB J. SAVORY 

*Fibre Optic Communication Systems Laboratory (FOCSLab), Electrical Engineering Division, Department of Engineering, University of Cambridge, 9 JJ Thomson Avenue, Cambridge CB3 0FA, UK*  
<sup>\*</sup>ms2688@cam.ac.uk

**Abstract:** Maximized information rates of ultra-wideband (typically, beyond 100-nm modulated bandwidth) lumped-amplified fiber-optic communication systems have been thoroughly examined accounting for the wavelength dependencies of optical fiber parameters in conjunction with the impact of the inelastic inter-channel stimulated Raman scattering (SRS). Three strategies to maximize point-to-point link throughput were proposed: optimizations of non-uniformly and uniformly distributed launch power per channel and the optimization based on adjusting to the target 3 dB ratio between the power of linear amplified spontaneous emission and nonlinear interference noise. The results clearly emphasize the possibility to approach nearly optimal system performance by means of implementing pragmatic engineering sub-optimal optimization strategies.

Published by Optica Publishing Group under the terms of the [Creative Commons Attribution 4.0 License](https://creativecommons.org/licenses/by/4.0/). Further distribution of this work must maintain attribution to the author(s) and the published article's title, journal citation, and DOI.

## 1. Introduction

Core optical networks undoubtedly play a substantial role in the entire digital communications infrastructure and the Internet. Over 95% of digital data traffic nowadays are carried over fiber-optic communication systems [1,2]. There also exist a tremendous growth in the demand of high information capacity giving rise to the so-called capacity crunch of optical fiber networks infrastructure, which commonly operates within the conventional *C*-band [3] spanned by the erbium-doped fiber amplifiers (EDFAs). Moreover, owing to the outbreak of COVID-19, a drastic increase in data transmission demands has also been recently observed. In spite of the fact that the overwhelming bulk of the world's fiber-optic communication systems have already undergone a long process of increasing engineering complexity and sophistication, and the information data rates of optical communication systems have already experienced an astonishing increase from 100 Mbps per fiber in the '70s to 10 Tbps in current commercial systems, however, the research challenges of maximizing the ultimate information capacity using standard single mode fibers (SMFs) still remain of much interest.

It is widely accepted that accommodating higher data rates poses greater requirements on optical modulated bandwidth in fiber-optic telecommunication systems. The opportunity to exploit the modulated bandwidth expansion might be a very promising short-term solution. Moreover, it is compatible, despite that it might be less power-efficient [4], with space-division multiplexing in terms of increasing future link throughput values to a Pbps range. Nonetheless, the detrimental effects, which inherently restrict the capacity of ultra-wideband (UWB) communication systems are the optical nonlinear effects occurred in silica fibers. These are the optical Kerr effect, which manifests itself as the four-wave mixing (FWM) among frequencies components in a

wavelength-division multiplexing (WDM) system, as well as the non-negligible inelastic inter-channel stimulated Raman scattering (SRS), which gives rise to the considerable differences in the performance of each individual WDM channel since lower frequency photons are amplified at expense of depleting energy of high frequency photons. These differences become even more substantial with increasing either the total input power or the entire modulated bandwidth [5–7]. As a consequence, the uniform launch power distributions (flat launch power profiles, i.e., the total optical input power is assumed to be equally split among all WDM channels), commonly used so far, cannot ultimately provide the best system performance. Thus, finding the appropriate launch power distributions maximizing the overall system performance is vital to enhance the ultimate system throughput.

This work is an extension of our recently published [8], where the point-to-point system throughput values were estimated through maximization of the total Shannon information rate in conjunction with further optimal allocation of the modulated bandwidth. Three optimization strategies were compared: the optimizations of non-uniformly and uniformly distributed launch power per channel, and the optimization based on adjusting to the ratio between the power of linear and nonlinear interference noise to 3 dB. These procedures were particularly realized by applying the global optimization algorithms, such as the algorithm (GA) [9] and the swarm intelligence based algorithms [10] enhanced by the gradient descent algorithm, returning the optimum launch power values of each individual channel across the whole transmit modulated bandwidth.

## 2. Modeling and optimization

### 2.1. UWB SMF parameters spectrum modeling

Optical fiber loss leading to the attenuation throughout optical signal propagation is one of the most detrimental effects observed in optical fiber communication systems. This occurs due to two main mechanisms in silica: Rayleigh scattering and infra-red absorption. It is additionally bounded by a  $\text{OH}^{-1}$  ions peak that can be accurately fitted via a superposition of four Lorentzian and one Gaussian function [11]. The value of carrier signal wavelength corresponding to the minimum fiber loss is mainly determined by the interplay between these two effects. The fiber attenuation coefficient  $\alpha$  [dB/km] can be approximately modeled as follows [11,12]

$$\alpha(\lambda) \approx \underbrace{A \left( \frac{\Lambda}{\lambda} \right)^4}_{\text{Rayleigh scattering}} + \underbrace{C \exp\left(-\frac{D}{\lambda}\right)}_{\text{IR absorption}} + \underbrace{\text{peaks}(\lambda)}_{[11]}, \quad (1)$$

where  $A$  and  $\Lambda$  are the Rayleigh scattering loss and wavelength, respectively;  $C$  and  $D$  are the absorption coefficients, which refer to the material property. Model Eq. (1) is shown in Fig. 1(a). A sufficiently accurate triangle approximation [13] of the normalized Raman gain coefficient  $g_R$  against the frequency separation (i.e., the frequency spacing among the WDM channels) was assumed, where the linear regression function with the Raman dispersion slope  $C_r$  is fitting the appropriate measurements of standard SMF-28 Fig. 1(b).

The spectrum of standard SMF chromatic dispersion  $D$  and dispersion slope  $S$  can be effectively modeled by applying the 4-term Sellmeier's fitting function:

$$D(\lambda) \approx B_1 \lambda^3 + B_2 \lambda + \frac{B_3}{\lambda^3} + \frac{B_4}{\lambda^5}, \quad S(\lambda) \triangleq \frac{dD(\lambda)}{d\lambda}, \quad (2)$$

where  $\{B_1, B_2, B_3, B_4\}$  are the appropriate set of the Sellmeier's coefficients.

The wavelength dependence of the fiber nonlinear coefficient  $\gamma$ , a main measure of Kerr nonlinearity in optical fibers, can be described as follows

$$\gamma(\lambda) \triangleq \frac{2\pi}{\lambda} \frac{n_2(\lambda)}{A_{\text{eff}}(\lambda)}, \quad (3)$$

where  $n_2$  is the nonlinear (Kerr) refractive index, which is a measure of the optical Kerr effect in silica media, and  $A_{\text{eff}}$  is the effective fiber mode area. Note that the variation of  $n_2$  is fairly negligible within the 1200 – 1400 nm telecommunication wavelength range and typically set to be constant (see Table 1). The effective fiber mode area represents the area of the fiber core would have if the optical power was assumed to be uniformly distributed across the fiber core, and it is, typically, of about  $A_{\text{eff}} \approx 80 \mu\text{m}^2$  at the center C-band wavelength of 1550 nm for SSMF that obviously may vary depending on the fiber design. Assuming that the transverse electric field amplitude component possesses a Gaussian shape, the wavelength dependency of fiber effective mode area can be given by the following empirical expression [14]

$$A_{\text{eff}}(\lambda) \approx \pi a^2 \left[ 0.65 + \frac{1.619}{V^{3/2}(\lambda)} + \frac{2.879}{V^6(\lambda)} \right]^2 \quad (1.2 \leq V \leq 2.4), \quad (4)$$

with  $a$  being the fiber core radius, and the  $V$ -value is thus defined as  $V(\lambda) = \frac{2\pi a}{\lambda} \cdot \text{NA}$ , where NA stands for the numerical aperture, i.e., the maximum angle measured outside the fiber with respect to the longitudinal direction of an incident beam that becomes confined within the fiber. Physically, the  $V$ -values defines the number of modes supported by the fiber. In order to support a single mode regime, the  $V$ -values should not exceed 2.405. It is worth noting that the empirical formula Eq. (4) approximates the exact solution to better than 1% accuracy. The values of all these parameters for standard SMF are provided in Table 1. The wavelength dependencies of optical fiber parameters and used for the calculations are shown in Fig. 1.

**Table 1. Standard SMF parameter values**

Parameters	Notations	Values	Units
Rayleigh scattering loss	$A$	1.7	dB/km
Rayleigh scattering wavelength	$\Lambda$	850	nm
IR absorption coefficient	$C$	$6.65 \times 10^{12}$	dB/km
IR absorption wavelength	$D$	52.62	$\mu\text{m}$
Sellmeier's coefficient	$B_1$	$1.529 \times 10^{-9}$	ps/nm <sup>4</sup> /km
–”–	$B_2$	0.017	ps/nm <sup>2</sup> /km
–”–	$B_3$	$-5.340 \times 10^{10}$	ps · nm <sup>2</sup> /km
–”–	$B_4$	$-7.700 \times 10^{15}$	ps · nm <sup>4</sup> /km
Step-index fiber core radius	$a$	4.1	$\mu\text{m}$
Fiber numerical aperture	NA	0.242	–
Fiber nonlinear (Kerr) refractive index	$n_2$	$2.80 \times 10^{-20}$	m <sup>2</sup> /W
Raman gain slope coefficient	$C_r$	0.0290	1/W/km/THz

## 2.2. UWB system performance modeling

The performance of dispersion-unmanaged ultra-wideband (UWB) optical communication systems can be evaluated by introducing the so-called effective receiver SNR. Since UWB SNR may exhibit significant variations across the entire spectrum, it is therefore customary to introduce

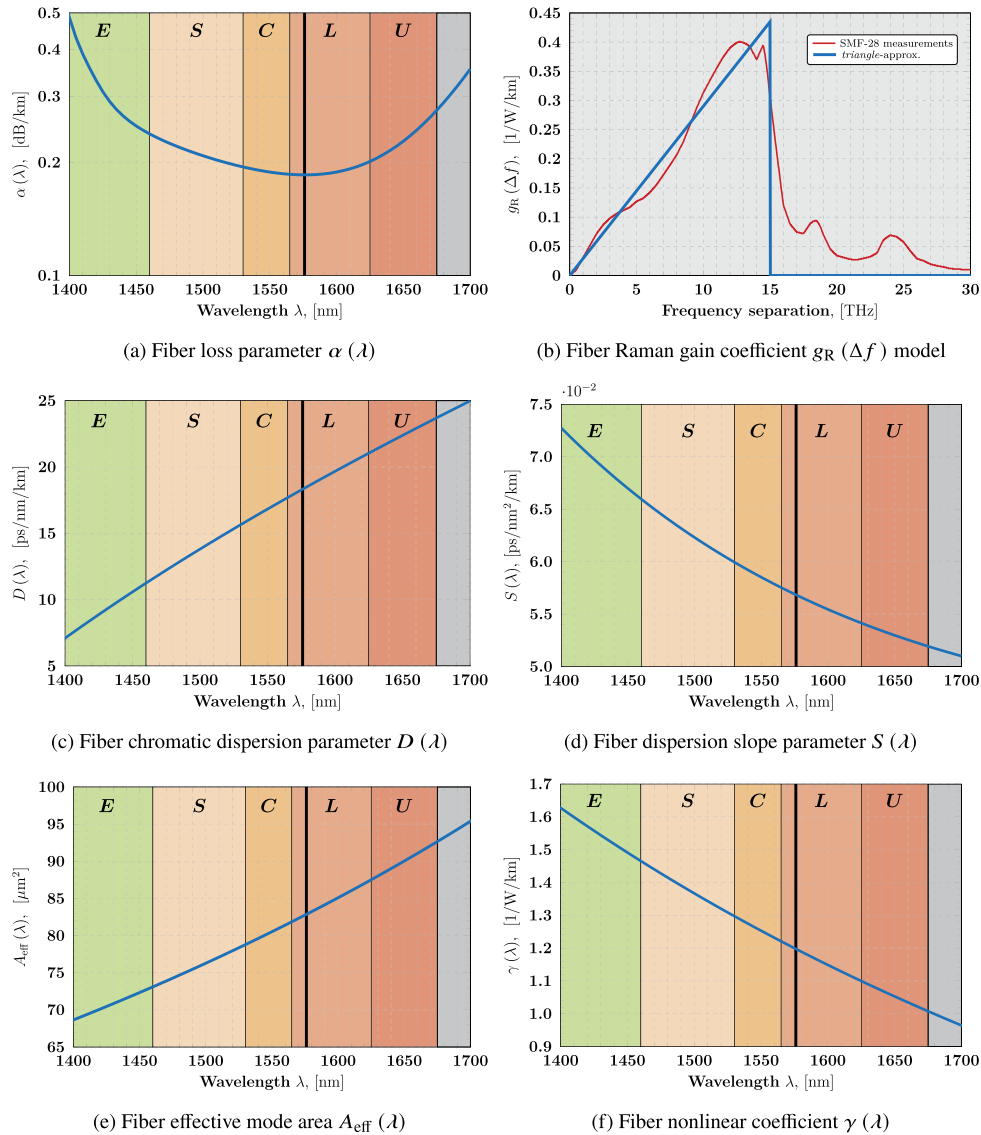


**Fig. 1.** Standard SMF parameters spectra: (a)  $\alpha(\lambda)$  is modeled by Eq. (1); (b) Triangle  $g_R$  approximation; (c)  $D(\lambda)$  is given by Eq. (2); (d)  $S(\lambda)$  in Eq. (2); (e)  $A_{\text{eff}}(\lambda)$  approximated by using (4); (f)  $\gamma(\lambda)$  is given by Eq. (3). The black vertical line indicates the minimum fiber loss wavelength  $\lambda_0 = 1576$  nm according to Eq. (1) model.

the frequency-dependent effective SNR per  $k$ -channel, which can be decomposed into locally white linear ASE noise and locally white nonlinear noise-like interference (NLI) contributions:

$$\text{SNR}[P(f_k)] = \left( \sigma_{\text{ASE}}^2(f_k) P^{-1}(f_k) + \eta(f_k) P^2(f_k) \right)^{-1}, \quad (5)$$

with  $f_k$  being the  $k$ -channel center frequency, and  $P(f_k)$  being the launch power spectral distribution with  $k$  being the channel index relative to the center bandwidth channel for which  $k = 0$ , and  $\sigma_{\text{ASE}}^2(f_k)$  being the linear noise power arisen by each EDFAs after each fiber span, and  $\eta(f_k)$  being the frequency-dependent factor that quantifies the amount of nonlinear interference. In UWB systems, the ASE noise is no longer white, moreover, it exhibits a nonlinear behavior (i.e., the power-dependency) due to the presence of the inelastic scattering. The frequency variation of ASE noise power reads [15]

$$\sigma_{\text{ASE}}^2(f_k) = N_s [G_{\text{EDFA}}(f_k) - 1] \cdot \text{NF}(f_k) \cdot (hf_0 + hf_k) \Delta f, \quad (6)$$

where  $N_s$  is the number of fiber spans, NF is the EDFA noise figure,  $\Delta f$  is the channel spacing,  $hf_k$  is the  $k$ -channel averaged photon energy. If both the fiber loss and the spectral tilt due to the inter-channel SRS effect are set to be entirely compensated and ideally equalized at each EDFA, hence, we have

$$G_{\text{EDFA}}(f_k) = e^{\alpha(f_k) \cdot L_s} \cdot G_{\text{SRS}}^{-1}(f_k). \quad (7)$$

with  $\alpha(f_k)$  being fiber loss parameter corresponding to the center frequency  $f_k$  of each  $k$ -channel, and  $L_s$  being the fibre span length. In the case of a uniform launch power spectral density (PSD), the SRS gain  $G_{\text{SRS}}$  can be closed-form approximated as follows [16]

$$G_{\text{SRS}}(f_k) \approx \frac{\exp(-f_k \cdot C_r L_{\text{eff}} P_{\text{tot}})}{\text{Sinhc}\left(\frac{\text{BW}}{2} \cdot C_r L_{\text{eff}} P_{\text{tot}}\right)}, \quad (8)$$

where  $\text{Sinhc}(x) \triangleq \frac{\sinh(x)}{x}$ , and  $\sinh(x)$  is the hyperbolic sine, and  $\text{rect}(x)$  is the rectangular function. The possibility to use the closed form approximation (8) improves significantly the computation time, however, it can only be effectively implemented for optimizing the uniformly distributed launch power, whereas a non-flat input power distribution admits the following approximate solution [17,18]

$$G_{\text{SRS}}(f_k) = \frac{P_{\text{tot}} \exp(-f_k \cdot C_r L_{\text{eff}} P_{\text{tot}})}{\sum_l P(f_k) \exp[-(f_k - f_l) \cdot C_r L_{\text{eff}} P_{\text{tot}}]}, \quad (9)$$

where the summation is taken over the entire bandwidth,  $C_r$  is the Raman gain slope,  $L_{\text{eff}}$  is the fiber effective length, and  $P_{\text{tot}}$  denotes the total launch power.

In order for estimating the NLI noise power in a Nyquist-spaced WDM system (i.e., it fulfills the Nyquist criterion, having a rectangular spectra of width  $\Delta f$  exactly equal to the symbol rate  $R_S$ ), one has to follow the perturbative GN model approach [19]. If the channel spacing is much smaller than total modulated BW, i.e.,  $\Delta f \ll \text{BW}$ , as well as the NLI is set to be locally flat, the NLI noise coefficient  $\eta$  can be modeled by applying the filtering of the NLI PSD  $S(\xi)$  Eq. (11) in the coherent receiver by means of a matched filter with a rectangular base-band function, it then

yields

$$\eta(f_k) = \frac{\gamma^2(f_k)}{\Delta f} \int_{\left(\frac{2k-1}{2}\right)\Delta f}^{\left(\frac{2k+1}{2}\right)\Delta f} d\xi \operatorname{rect}\left(\frac{\xi}{\Delta f}\right) \cdot S(\xi), \quad (10)$$

where the NLI PSD  $S(\xi)$  is given by [19]

$$S(\xi) \approx \frac{16}{27 R_S^2} \int_{-\infty}^{\infty} \int_{-\infty}^{\infty} df_1 df_2 \operatorname{rect}\left(\frac{f_1 + f_2 - \xi}{\text{BW}}\right) \cdot |\rho(\xi, f_1, f_2 | L_s)|^2, \quad (11)$$

with the symbol rate  $R_S$ . The appropriate FWM efficiency factor is defined as follows

$$\rho(f_k, f_1, f_2 | L_s) = \int_0^{L_s} d\zeta e^{i\Delta\beta(f_k, f_1, f_2)\zeta} \cdot \Delta\rho(f_k, f_1, f_2, | \zeta), \quad (12)$$

where the impact of inter-channel SRS effect is implicitly taken into account by the signal power distance evolution factor  $\Delta\rho(f_k, f_1, f_2 | \zeta)$  that is introduced and well-described in, e.g., [5,6], and  $\Delta\beta$  is the FWM phase-mismatch factor that can be approximated by including the dispersion slope as follows (see, e.g., [20])

$$\begin{aligned} \Delta\beta(f, f_1, f_2) &= \beta(f_1 + f_2 - f) - \beta(f_1) - \beta(f_2) + \beta(f) \\ &\approx 4\pi^2 [\beta_2 + \pi(f_1 + f_2)\beta_3] \cdot (f_1 - f)(f_2 - f), \end{aligned} \quad (13)$$

with  $\beta(\cdot)$  being the real part of the propagation constant of light (i.e., the phase shift) as a function of frequency, and the fiber chromatic dispersion and dispersion slope are captured by the second-order  $\beta_2$  and the third-order  $\beta_3$  group-velocity dispersion coefficients in the Taylor expansion, respectively.

### 2.3. Maximized information throughput approaches

In this section, we describe some numerical techniques to maximize the capacity of point-to-point fiber-optic links by optimizing the launch power per channel profile and allocating the modulated signal bandwidth. These optimization problems are overcome by means of applying the global optimization algorithms, such as the genetic (GA) and the PSO algorithms, which adjust the optimum launch power values of each individual channel across the whole modulated bandwidth.

#### 2.3.1. Maximizing Shannon rate throughput

Finding optimal launch power distribution shapes  $P_{\text{opt}}(f_k)$ , which maximize the overall information rate implies the unconstrained optimization problem, it thus reads

$$P_{\text{opt}}(f_k) = \arg \max_{P(f_k) : \lambda_0 = \text{const}} \left\{ \sum_k C[P(f_k) | \lambda_0] \right\}, \quad (14)$$

where the maximization is taken over all possible unconstrained launch power per channel values at each fixed value of the reference center BW wavelength  $\lambda_0$ . It is worth noting that the global unconstrained launch power optimization was independently carried out by using both the GA [9] and the particle swarm optimization (PSO) algorithm [10] enhanced by the gradient descent optimization algorithm. The functional  $C$  in (14) defines the  $k$ -channel Shannon information

rate, which defines the Gaussian channel capacity upper bound measured in bits per channel use, it thus yields

$$C [ P ( f_k ) | \lambda_0 ] \triangleq 2 \log_2 \left( 1 + \text{SNR} [ P ( f_k ) | \lambda_0 ] \right). \quad (15)$$

The corresponding throughput  $T^*$  measured in [bit/s] can be obtained by optimizing the launch power profile is therefore given by

$$T^* (\lambda_0) = R_S \sum_k C [ P_{\text{opt}} ( f_k ) | \lambda_0 ]. \quad (16)$$

Finally, the further system performance improvement can be attained via allocating the transmit modulated bandwidth by varying its center wavelength, and therefore, the ultimate point-to-point link throughput  $T$  can be mathematically expressed as follows

$$T = \max_{\lambda_0} T^* (\lambda_0). \quad (17)$$

### 2.3.2. Pragmatic engineering optimization approaches

In this section, we suggested two pragmatic optimization methods, such as the heuristic 3-dB ASE/NLI ratio based approach and the uniform sub-optimal flat power optimization.

From an engineering standpoint, there might be a more pragmatic approach to make an adjustment of launch power per channel values in UWB multi-channel systems, which is based on the 3 dB ratio between the power of linear ASE and the NLI noise. This approach is certainly sub-optimal since it comes from the conventional flat spectrum assumption. In other words, to end up with sub-optimal non-uniform launch power profiles, one needs to force the ASE/NLI noise power ratio to be equal to 3 dB, which can be technically realized by numerically minimizing the Euclidean distance to approach the 3-dB target, it reads

$$P_{\text{opt}}^{(3\text{dB})} (\lambda_k) = \arg \min_{P(\lambda_k)} \left\| 2 - \frac{\sigma_{\text{ASE}}^2 [ P(\lambda_k) ]}{\eta [ P(\lambda_k) ] \cdot P^3(\lambda_k)} \right\|_2, \quad (18)$$

where  $\|\cdot\|_2$  denotes  $\ell_2$ -norm (i.e., the Euclidean norm).

Besides the non-uniform optimal launch Eq. (14) that requires to deal with a multi-dimensional optimization problem, the optimal flat launch power is much less computationally expensive, and can be found by solving the one-dimension problem:

$$P_{\text{flat}} ( f_k ) = \arg \max_{P_{\text{flat}} : \lambda_0 = \text{const}} \left\{ \sum_k C [ P_{\text{flat}} | \lambda_0 ] \right\}, \quad (19)$$

where  $P_{\text{flat}} = \text{const}$  denotes the frequency-independent power level per channel.

## 3. Results and discussion

In order to properly estimate the performance of fiber-optic systems with a modulated bandwidth beyond 100 nm (i.e., beyond  $(C + L)$ -band), apart from the non-negligible inter-channel SRS effect, a proper consideration and modeling of the wavelength dependencies of single mode optical fiber parameters become also essential. Figure 1 illustrates the the fiber parameters spectra, such as the fiber loss (a), the Raman gain coefficient (b) the chromatic dispersion and dispersion slope (c,d), the fiber effective mode area and the fiber nonlinear coefficient (e,f). These variations were quantified within a range of 1450 – 1750 nm. The monotonic behavior of the fiber parameters spectra has been observed except for the fiber loss profile, where the value of minimum loss wavelength is set to a WDM carrier. It is worth emphasizing that for UWB systems,

the carrier wavelength is no longer corresponding to the conventional center *C*-band 1550 nm wavelength. In addition, within the framework of our analytical approach, the spectral gaps between *S*, *C* and *L* were omitted. Without loss of generality, we have considered an ideal 100 GBd polarization-multiplexed Nyquist-spaced WDM fiber-optic transmission system (Table 2) over up to 25 THz modulated bandwidth at the carrier wavelength corresponding to the minimum fiber loss according to the model given by Eq. (1). All fiber spans and lumped EDFAs are assumed to be identical with a length of  $L_s = 100$  km and the EDFA noise figure of  $NF = 4.5$  dB (Table 2). Note that our analytical approach can be straightforwardly generalized by examining amplifier physics (see, e.g., [21]), as well as adding practical limitations and imperfections on the real-world amplification schemes, such as considering residual transceiver impairments, piecewise-defined amplifier NF spectrum, amplifier gain spectral slope, gain ripples, spectral gaps, etc.

**Table 2. Fiber-optic system parameter values**

Parameters	Notations	Values	Units
Symbol rate	$R_S$	100	GBd
WDM channel spacing	$\Delta f$	100	GHz
EDFA noise figure	NF	4.5	dB
Fiber span length	$L_s$	100	km
Total number of spans in a link	$N_s$	12	–

Following the perturbative GN model approach originally derived in [19], the expression of effective SNR Eq. (5), the linear ASE noise Eq. (6), and the NLI Eq. (10) now take into account both the wavelength variations of fiber parameters and the impact of SRS effect.

Figure 2 shows a family of numerically optimized launch power per channel distributions, which maximize the system throughput at a fixed value of the center wavelength. The optimization strategies were compared, such as the non-uniform power per channel distribution requiring the adjustment of each individual channel power, the so-called “3-dB rule” approach based on optimizing the non-uniform profile by forcing the ratio between ASE noise power and the power of NLI to the target 3-dB ratio, and the uniform flat power level optimization assuming the same power per channel across the entire bandwidth. Here it should be mentioned that the uniform flat power level optimization substantially reduces the multi-dimensional optimization problem to one-dimensional one, which is much less numerically expensive, and thus, significantly saves overall computational time. Notably, all these power profiles remain convex function, unless the impact of SRS is significant. However, with an increase in the number of WDM channels (i.e.,  $N_{ch} \geq 201$ ), the combination of the FWM Gaussian noise-like distortions and the Raman gain gives rise to non-convex numerical solutions. Figure 3 shows the scaling between the launch power-optimized link throughput at a given center wavelength. It also indicates that the information loss due to the presence of inter-channel SRS monotonically increases with the number of WDM channels, e.g., it may achieve of about 13.5% at 25 THz modulated bandwidth. This figure additionally illustrates that assuming the SRS spectral tilt is entirely equalized at every fiber span the optimal system throughput can be nearly approached by operating with the pragmatic sub-optimal optimization strategies, which, in turn, may substantially simplify the computation complexity. In particular, at about 25 THz modulated bandwidth, the difference between the throughput obtained by the non-uniformly optimized launch power, and the strategy of 3-dB ASE/NLI ratio and simplistic uniform launch power optimization are about 8% and 5%, respectively. This accuracy might be fairly acceptable for engineering applications, when the trade-off between complexity and accuracy becomes essential. It should also be pointed out that the aforementioned “3-dB rule” power optimization strategy work well up to about 17.5

THz bandwidth. Figure 3 indicates 3-dB rule is a sensible option provided less than 175 WDM channels.

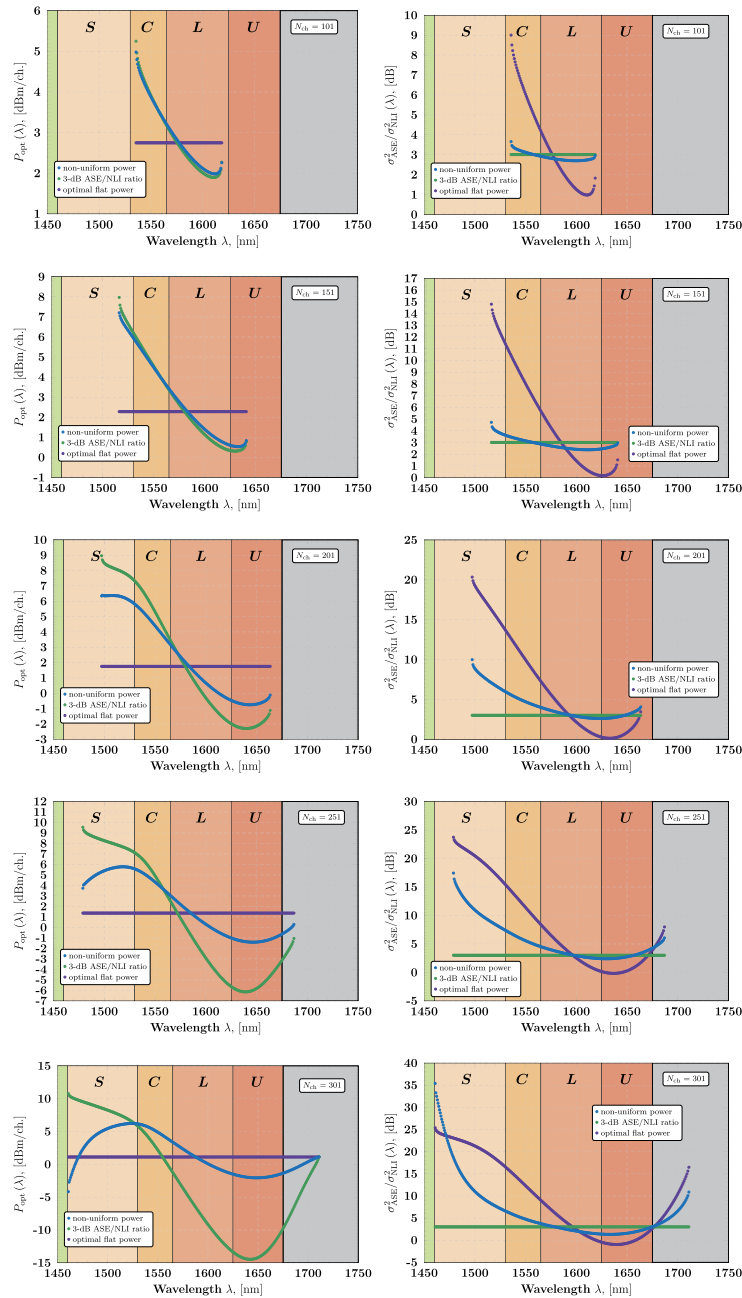


**Fig. 2.** Optimized launch power profiles and the corresponding ratio between the ASE noise and NLI noise.

Finally, the further system performance improvement can be attained via allocating the transmit modulated bandwidth by varying the WDM carrier wavelength. Figure 4 shows that the maximized throughput obtained by optimizing the launch power profiles exhibits a strictly

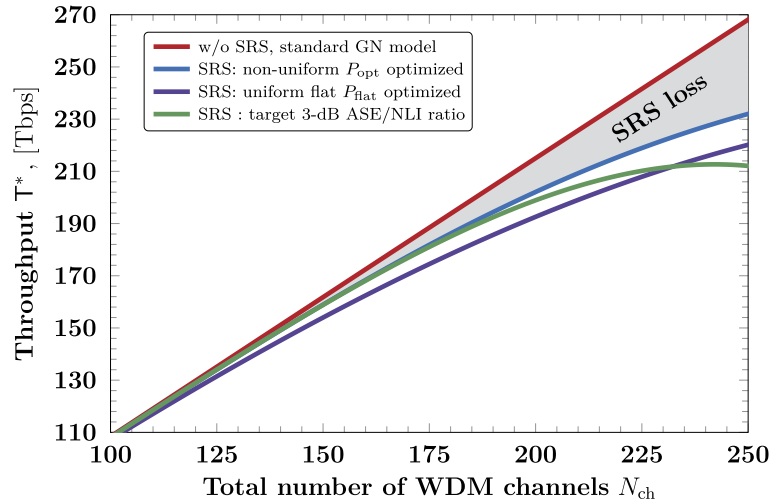


**Fig. 3.** Scaling between the launch power-optimized link throughput  $T^*$  (see, Eq. (16)) and the total number of 100 GHz Nyquist-spaced WDM channels at the minimum fiber loss carrier wavelength  $\lambda_0 = 1576$  nm considering three optimization strategies with launch power distribution determined by Eqs. (14), (19), and (18) for non-uniform, uniform flat, and target 3-dB ASE/NLI noise power ratio, respectively.

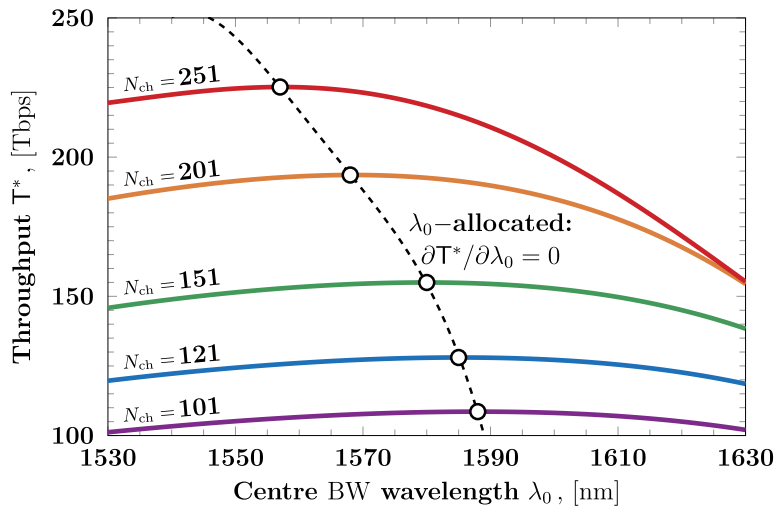


**Fig. 4.** System throughput  $T^*$  after uniform flat launch power optimization given by Eq. (19) as function of the center bandwidth wavelength  $\lambda_0$  for different number of WDM channels  $N_{ch}$  with a channel spacing of 100 GHz each. The dashed black line indicates the values of the wavelength defining the optimal allocation of modulated bandwidth to maximize the throughput.

concave behavior with respect to the center-channel wavelength. It is also observed that the allocated values of  $\lambda_0$  corresponding to the maximum values of throughput  $T^*$  in Eq. (16) are shifting to lower wavelength values with increasing the total number of WDM channels. As shown in Fig. 5, the system performance increment obtained due to bandwidth allocation in the case of the standard GN model approach (i.e., in the absence of both the chromatic dispersion slope and SRS) remains constant and marginal (less than 1%). However, at 25 THz modulated

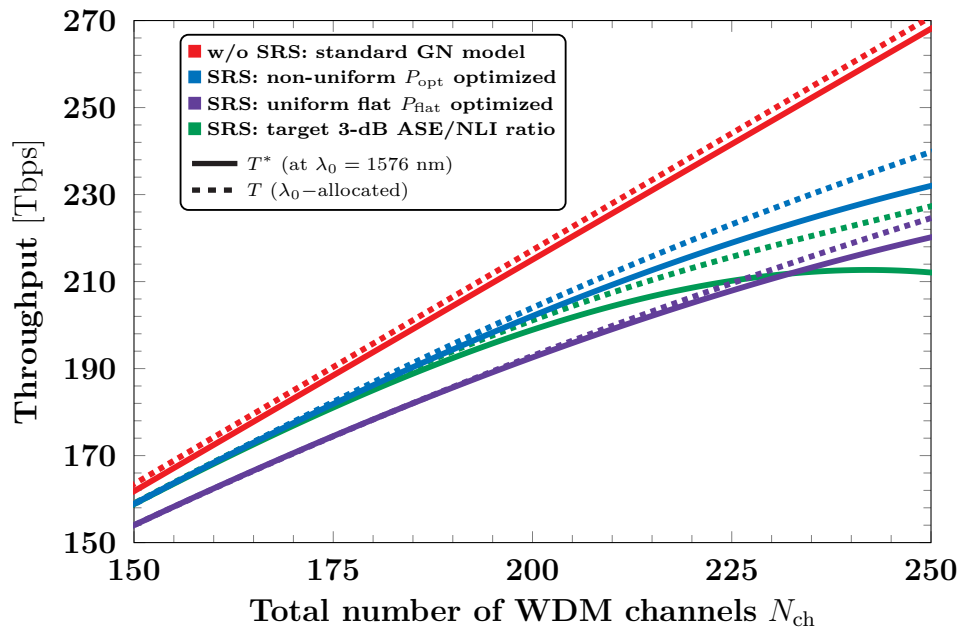


**Fig. 5.**  $\lambda_0$ -allocated scaling given by Eq. (17) between the link throughput  $T^*$  and the total number of 100 GHz Nyquist-spaced WDM channels.

bandwidth, in the case of non-uniform, uniform flat, and “3-dB rule” power optimization strategies including both the effect of dispersion slope and inter-channel SRS, it can theoretically reach up to 4%, 3% and 7%, respectively. It can also be distinctly observed that optimally allocating modulation bandwidth may give more benefits with increasing the number of WDM channels. In all cases, the global unconstrained launch power optimizations were carried out by independently implementing the GA and the PSO algorithms, which were additionally enhanced by the gradient descent optimization algorithm.

#### 4. Conclusion

This work examines the bounds on the scaling between the ultimate point-to-point UWB WDM standard SMF link throughput and the total number of channels in an ideal Nyquist-spaced WDM transmission system. These bounds were numerically evaluated by implementing both the optimization of launch power per channel distribution and the UWB allocation. In addition, we make use of some pragmatic sub-optimal but practically relevant optimization strategies, which simplify numerical complexity and may admit nearly optimal solutions. Some extra benefits were also attained via modulation bandwidth allocation. Such analytical models and optimization techniques are vital to accurately estimate and to optimize UWB fiber-optic system performers within reasonable times. Moreover, it provides a certain insight into the estimation of quality-of-transmission (QoT) in the context of future UWB optical networks. The evaluation of the system capacity spectral ripples, as well as a proper exploration and implementation of amplifier physics are left for further investigation.

**Funding.** Authors thank BT (British Telecommunications) and Huawei for funding through the High Capacity Transmission Systems project and Engineering and Physical Sciences Research Council funding through the TRANSNET project with grant ID (EP/R035342/1); .

**Acknowledgments.** The authors would like to thank Yann Frignac, Ivan Fernandez de Jauregui Ruiz and Gabriel Charlet from Huawei Technologies Paris, and Md Asif Iqbal and Andrew Lord from BT for brainstorming sessions and insightful discussions.

**Disclosures.** The authors declare that there are no conflicts of interest related to this article.

**Data availability.** Data underlying the results presented in this paper are not publicly available at this time but may be obtained from the authors upon reasonable request.

## References

1. Cisco. "Cisco Visual Networking Index: Forecast and Methodology 2017-2022," [https://www.cisco.com/c/dam/m/en\\_us/network-intelligence/service-provider/digital-transformation/knowledge-network-webinars/pdfs/1213-business-services-ckn.pdf](https://www.cisco.com/c/dam/m/en_us/network-intelligence/service-provider/digital-transformation/knowledge-network-webinars/pdfs/1213-business-services-ckn.pdf) (2018).
2. P. Bayvel, R. Maher, T. Xu, G. Liga, N. A. Shevchenko, D. Lavery, A. Alvarado, and R. I. Killey, "Maximizing the optical network capacity," *Phil. Trans. R. Soc. A*, **374**(2062), 20140440 (2016).
3. A. Chralyvy, "Plenary paper: The coming capacity crunch," in *2009 35th European Conference on Optical Communication*, (IEEE, 2009), pp. 1.
4. P. J. Winzer, "Would scaling to extreme ultraviolet or soft X-ray communications resolve the capacity crunch?" *J. Lightwave Technol.* **36**(24), 5786–5793 (2018).
5. I. Roberts, J. M. Kahn, J. Harley, and D. W. Boertjes, "Channel power optimization of WDM systems following Gaussian noise nonlinearity model in presence of stimulated Raman scattering," *J. Lightwave Technol.* **35**(23), 5237–5249 (2017).
6. M. Cantono, D. Pileri, A. Ferrari, C. Catanese, J. Thouras, J.-L. Augé, and V. Curri, "On the interplay of nonlinear interference generation with stimulated Raman scattering for QoT estimation," *J. Lightwave Technol.* **36**(15), 3131–3141 (2018).
7. D. Semrau, R. I. Killey, and P. Bayvel, "The Gaussian noise model in the presence of inter-channel stimulated Raman scattering," *J. Lightwave Technol.* **36**(14), 3046–3055 (2018).
8. N. A. Shevchenko, S. Nallaperuma, and S. J. Savory, "Ultra-wideband information throughput attained via launch power allocation," in *2021 International Conference on Optical Network Design and Modeling (ONDM)*, (IEEE, 2021), pp. 1–3.
9. A. E. Eiben and J. E. Smith, *Introduction to evolutionary computing*, vol. 53 (Springer, 2003).
10. R. Eberhart and J. Kennedy, "A new optimizer using particle swarm theory," in *MHS'95. Proceedings of the Sixth International Symposium on Micro Machine and Human Science*, (Ieee, 1995), pp. 39–43.
11. M. Bredol, D. Leers, L. Bosselaar, and M. Hutjens, "Improved model for OH absorption in optical fibers," *J. Lightwave Technol.* **8**(10), 1536–1540 (1990).
12. M. Ohashi, K. Shiraki, and K. Tajima, "Optical loss property of silica-based single-mode fibers," *J. Lightwave Technol.* **10**(5), 539–543 (1992).
13. A. R. Chraplyvy, "Optical power limits in multi-channel wavelength-division-multiplexed systems due to stimulated Raman scattering," *Electron. Lett.* **20**(2), 58–59 (1984).
14. D. Marcuse, "Loss analysis of single-mode fiber splices," *Bell Syst. Tech. J.* **56**(5), 703–718 (1977).
15. C. R. Giles and E. Desurvire, "Modeling erbium-doped fiber amplifiers," *J. Lightwave Technol.* **9**(2), 271–283 (1991).
16. M. Zirngibl, "Analytical model of Raman gain effects in massive wavelength division multiplexed transmission systems," *Electron. Lett.* **34**(8), 789–790 (1998).
17. D. N. Christodoulides and R. B. Jander, "Evolution of stimulated Raman crosstalk in wavelength division multiplexed systems," *IEEE Photonics Technol. Lett.* **8**(12), 1722–1724 (1996).
18. L. B. Djordjevic, A. Stavdas, C. Skoufis, S. Sygletos, and C. Matrakidis, "Analytical modelling of fibre nonlinearities in amplified dispersion compensated WDM systems," *Int. J. Of Model. Simul.* **23**(4), 226–233 (2003).
19. P. Poggiolini, "The GN model of non-linear propagation in uncompensated coherent optical systems," *J. Lightwave Technol.* **30**(24), 3857–3879 (2012).
20. W. Zeiler, F. Di Pasquale, P. Bayvel, and J. E. Midwinter, "Modeling of four-wave mixing and gain peaking in amplified WDM optical communication systems and networks," *J. Lightwave Technol.* **14**(9), 1933–1942 (1996).
21. J. K. Perin, J. M. Kahn, J. D. Downie, J. Hurley, and K. Bennett, "Importance of amplifier physics in maximizing the capacity of submarine links," *J. Lightwave Technol.* **37**(9), 2076–2085 (2019).